Journal of Automation and Intelligence 3 (2024) 160–168

Contents lists available at ScienceDirect

Journal of Automation and Intelligence

journal homepage: www.keaipublishing.com/en/journals/journal-of-automation-and-intelligence/

Research article

Fast and robust strain signal processing for aircraft structural health monitoring☆

Cong Wang [a,b], Xin Tan [a], Xiaobin Ren [c,*], Xuelong Li [d]

[a] School of Artificial Intelligence, OPtics and ElectroNics (iOPEN), Northwestern Polytechnical University, Xi'an, 710072, China
[b] Research & Development Institute of Northwestern Polytechnical University in Shenzhen, Shenzhen, 518063, China
[c] Shaanxi Neifu Zhongfei Airport Management Co., Ltd., Xi'an, 710061, China
[d] Institute of Artificial Intelligence (TeleAI), China Telecom., Beijing, 100033, China

ARTICLE INFO

Keywords:
Structural health monitoring
Signal processing
Abnormal judgment
Noise analysis
Total variation

ABSTRACT

This work elaborates a fast and robust structural health monitoring scheme for copying with aircraft structural fatigue. The type of noise in structural strain signals is determined by using a statistical analysis method, which can be regarded as a mixture of Gaussian-like (tiny hairy signals) and impulse-like noise (single signals with anomalous movements in peak and valley areas). Based on this, a least squares filtering method is employed to preprocess strain signals. To precisely eliminate noise or outliers in strain signals, we propose a novel variational model to generate step signals instead of strain ones. Expert judgments are employed to classify the generated signals. Based on the classification labels, whether the aircraft is structurally healthy is accurately judged. By taking the generated step count vectors and labels as an input, a discriminative neural network is proposed to realize automatic signal discrimination. The network output means whether the aircraft structure is healthy or not. Experimental results demonstrate that the proposed scheme is effective and efficient, as well as achieves more satisfactory results than other peers.

1. Introduction

Structural health monitoring is an in-situ and online structure detection method for aircraft structural damage [1–4]. In many countries, such as the United States and China, aviation regulations require rigorous durability and damage tolerance tests for critical aircraft structures that could potentially cause substantial harm to aircrafts [5,6]. Aircraft structural strain sensors play an important role in the fatigue damage testing of aircraft structures [7,8]. Under normal circumstances, structural health monitoring needs to transmit strain signals produced by such sensors, as well as analyze, process, and predict them [9–12].

In real-world damage tolerance tests, strain signals are characterized by a large number of measurement channels and operating conditions. Due to complex manufacturing process and working condition, they usually have two distinct characteristics, i.e., irregularity and diversity. Irregularity means that the output signal length of various strain sensors is different due to different strain generation conditions. Diversity signifies that strain signals are of various forms and values vary greatly due to large differences in stresses on different structures of an aircraft. Intuitively, Fig. 1 shows normal and abnormal strain signals. The curve in Fig. 1(a) represents that the aircraft is structurally healthy. On the contrary, one in Fig. 1(b) indicates aircraft's structural unhealthy.

In addition to the above two cases, there are many strain signals with different shapes, through which it is not easy to determine whether the aircraft structure is healthy, as shown in Fig. 2. There exist a lot of outliers and noise in these irregular signals. They put forward high requirements for the design of structural health monitoring methods. Especially, it is extremely important and necessary to perform noise analysis and anomaly determination on these irregular strain signals.

In the existing studies for aircraft structural health monitoring, researchers pay more attention to system architecture design [13,14], aircraft smart skin [15], composite materials [16,17], and optical sensors applications [18,19]. To the best of our knowledge, there are only a few studies implement aircraft structural health monitoring by means of strain signal processing [20–22]. For instance, Al-Salah et al. [20]

Peer review under responsibility of Chongqing University.

☆ This work was supported in part by the National Natural Science Foundation of China under Grant No. 62206220, in part by the Young Talent Fund of Association for Science and Technology in Shaanxi, China under Grant No. 20230140, in part by the Guangdong Basic and Applied Basic Research Foundation, China under Grant No. 2021A1515110019, in part by the Chunhui Program of Ministry of Education of China under Grant No. HZKY20220537, and in part by the Fundamental Research Funds for the Central Universities, China under Grant No. G2023KY0601.

* Corresponding author.
E-mail addresses: congwang0705@nwpu.edu.cn (C. Wang), tan6xin@gmail.com (X. Tan), 174455730@qq.com (X. Ren), xuelong_li@ieee.org (X. Li).

https://doi.org/10.1016/j.jai.2024.07.001
Received 29 May 2024; Received in revised form 22 June 2024; Accepted 2 July 2024
Available online 5 July 2024

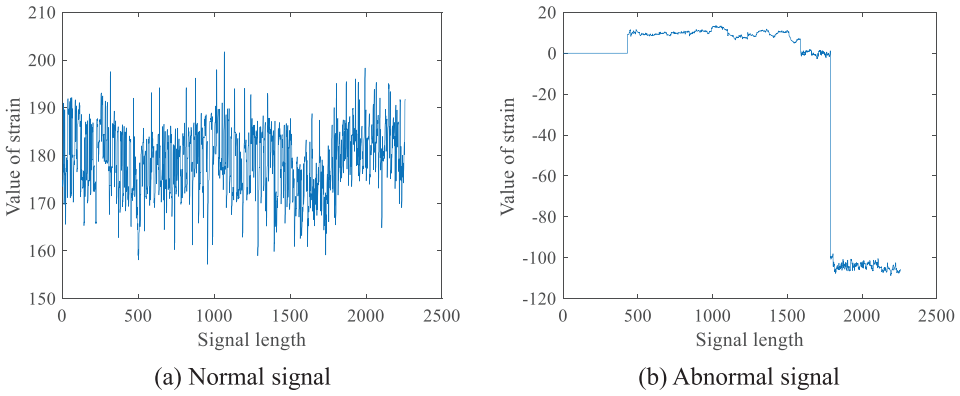

Fig. 1. Normal and abnormal strain signals.

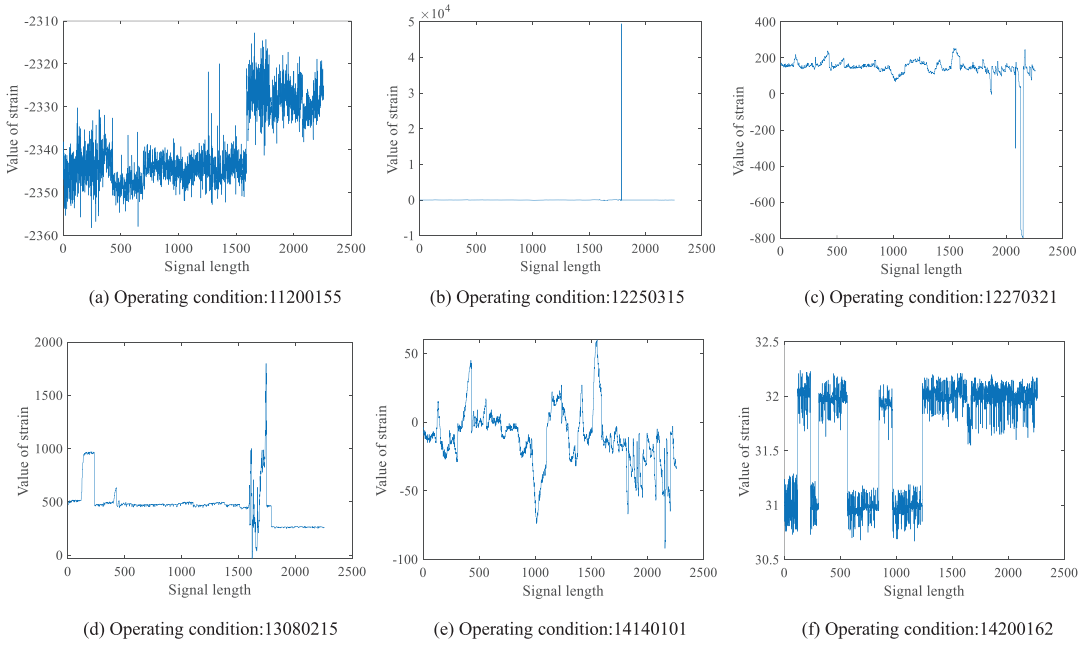

Fig. 2. Six randomly sampled strain signals under an aircraft type.

develop and implement a clustering and classification software system for aircraft structural health monitoring. The system is divided into three modules, i.e., feature extraction, clustering and classification, and decision-fusion module. More recently, Du et al. [22] report a heterogeneous structural response prediction framework based on deep learning model, which makes full use of spatial and temporal correlations of structural response. The correlation between heterogeneous responses is also mined. However, the above methods rely more on the good performance of hardware systems and the intervention of expert experience so as to realize aircraft structural health monitoring.

With the development of computer technologies, the number of time-series signal processing methods is increasing and becoming more and more mature, including adaptive filtering [23–26], wavelet denoising [27–30], sparse representation [31–33], and machine learning methods [34–36]. Especially in the last few years, deep learning methods, such as convolutional neural networks (CNN) [37,38], recurrent neural networks (RNN) [39], and long-short term memory networks (LSTM) [40], have achieved better results in various time-series signal processing tasks. Such methods utilize the powerful fitting ability and adaptive learning capability of neural networks to effectively model and cope with complex signal noise [41]. However, their training and tuning processes require a large amount of computational costs. For small samples or less labeled data, their may suffer from overfitting problems. In addition, due to the data complexity of aircraft structural strain signals, the robustness of single signal denoising methods are greatly reduced so that they may not be able to accurately judge whether the aircraft is structurally healthy.

To overcome these difficulties, this work elaborates a fast and robust structural health monitoring scheme and achieve accurate judgment of aircraft structural health. A brief framework of the proposed scheme is portrayed in Fig. 3. Intuitively, such scheme consists of five stages. The type of noise in strain signals is first determined by using a statistical analysis method, which can be regarded as a mixture of Gaussian-like (tiny hairy signals) and impulse-like noise (single signals with anomalous movements in peak and valley areas). Based on this, a least squares filtering method [42] is employed to preprocess strain signals. To precisely eliminate noise or outliers in strain signals, we propose a novel total variational model to generate step signals by only adjusting parameter α. Whereafter, expert judgments are employed to classify the generated signals. Based on the classification labels, whether the

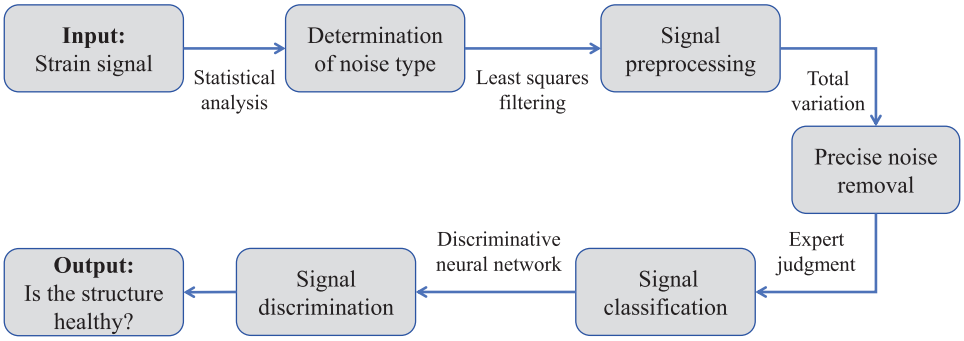

Fig. 3. Framework of the proposed multi-strategy scheme.

aircraft is structurally healthy is accurately judged. By taking the generated step count vectors and labels as a network input, a discriminative neural network is proposed to realize a signal discrimination stage. Finally, the network output means whether the aircraft structure is healthy or not.

In summary, this work makes three contributions as follows:

- It proposes a statistical analysis method to determine the noise type in strain signals, i.e., a mixture of Gaussian-like (tiny hairy signals) and impulse-like noise (single signals with anomalous movements in peak and valley areas). This sets the stage for preprocessing the signals by a least squares filtering method.
- It develops a novel variational model and minimization algorithm for precise noise removal, which transforms complex strain signals into simple step ones. By counting the steps and expert judgments, whether the aircraft is structurally healthy is accurately judged.
- It establishes a discriminative neural network to realize automatic signal discrimination. The network structure is simple and easy to train. The network output means whether the aircraft structure is healthy or not.

The originality of this paper is to propose a multi-strategy scheme so as to realize fast and robust structural health monitoring, which greatly reduces the safety risks caused by aircraft structural fatigue. Under the influence of unknown noise and complex signal condition, such scheme achieves effective noise removal and accurate judgment of aircraft structural health. Its success is mainly attributed to the proposed variational model, which transforms the complex strain signal into a simple step count vector, so that the data dimensionality is greatly reduced and the judgment accuracy is improved.

The remainder of this paper is organized as follows. Section 2 formulates the proposed methodology. Section 3 reports experimental results. The relevant conclusions are summarized in Section 4.

2. Proposed methodology

2.1. Statistical analysis method

Due to various interferences existing in the acquisition process of strain signals or measurement process of strain sensors, an observed strain signal inevitably contains noise or outliers. Formally speaking, it can be expressed as

$$y(t) = u(t) + n(t)$$

where t represents the sampling time, $u(t)$ is a noise-free strain signal, and $n(t)$ is the noise or outlier. In this work, we apply a statistical analysis method to determine $n(t)$. Specifically, the statistical analysis method uses a variety of signal filtering methods, including Gaussian filtering, mean filtering and removal of outliers, to process the observed strain signal. Its framework diagram is shown in Fig. 4.

The filtered signal is compared with the original strain signal, and the noise contained in the signal can be roughly determined by comparing in the signal peak or valley fluctuation region and the signal flat region. When the peak or valley fluctuation of the strain value exceeds 80, the signal contains impulse noise n_1. We denote the difference of the observed signal data and Gaussian filtering results in a smooth region as n_2. If 80% of n_2 is not equal to 0 and $-10 \le n_2 \le 10$, we determine that the observed signal contains Gaussian noise, i.e., n_2. Thus, n can be expressed as

$$n = n_1 + n_2 + \cdots + n_\beta$$

where β indicates the noise type count.

2.2. Total variational model and minimization algorithm

In a discrete domain $t = 1, 2, \ldots, N$, we consider an observed signal $y = [y_1, y_2, \ldots, y_N]^{\mathrm{T}}$. The gradient operator on noise-free signal u can be denoted as $\nabla u = [\vec{d}_1, \vec{d}_2, \ldots, \vec{d}_N]^{\mathrm{T}}$, where $\vec{d}_i$ denotes the gradient of signal u at position i. The task of signal denoising is to approximate

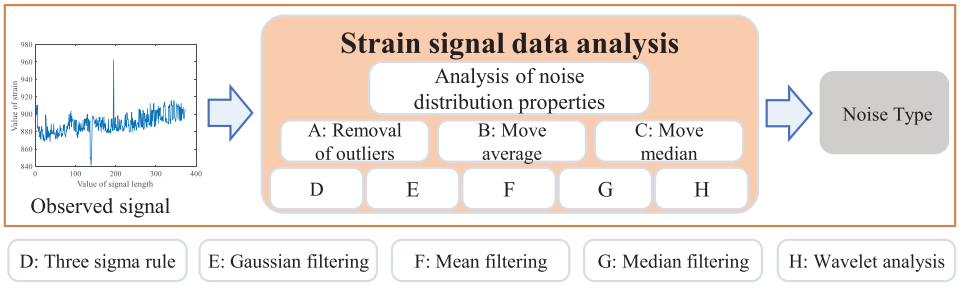

Fig. 4. Framework of statistical analysis method for noise analysis.

the true underlying signal u from y. Therefore, we propose a total variational model and define its energy function $E(u)$ as

$$E(u) = \alpha \cdot \Gamma(u) + D(u) \tag{1}$$

where $D(u)$ and $\Gamma(u)$ are fidelity and regularization terms, respectively. They are formulated as

$$D(u) = \sum_{i=1}^{N} \gamma_i \left| u_i - y_i \right|, \ \Gamma(u) = \sum_{i=1}^{N} \left\| \nabla u_i \right\|_1$$

The fidelity term $D(u)$ is used to keep the true underlying signal u consistent with the observed data. The smoothing term $\Gamma(u)$ is used to encourage the smoothness of the signal u. Here, α is a weight coefficient between both terms, which is used to balance them. We transform signal denoising into solving an optimization problem. The objective is to minimize the energy function $E(u)$:

$$\begin{aligned} \hat{u} &= \arg\min_{u} E(u) \\ &= \arg\min_{u \in \mathbb{R}^N} \alpha \sum_{i=1}^{N-1} |u_i - u_{i+1}| + \sum_{i=1}^{N} \gamma_i |u_i - y_i| \end{aligned} \tag{2}$$

where $\hat{u}$ is a solution to optimization problem (2) and the ℓ_1-TV generalization for observed data $y \in \mathbb{R}^N$ as

$$R_{\alpha;y}(u) = \alpha \sum_{i=1}^{N-1} d(u_i, u_{i+1}) + \sum_{i=1}^{N} \gamma_i d(u_i, y_i)$$

where d denotes the ℓ_1-norm distance between two points in the corresponding data space. The weight vector γ is used to account for non-isometric sampling. This means that the data $y_i = f(t_i)$ is a continuous signal f sampled at the non-equidistant points $t_1 < t_2 < \cdots < t_N$. A reasonable value of γ_i is the average distance from the sampling point t_i to its neighboring points t_{i-1} and t_{i+1}, i.e., $\gamma_i = (t_i - t_{i-1} + t_{i+1} - t_i)/2 = (t_{i+1} - t_{i-1})/2$. In this paper, we use equidistant sampling so as to have $\gamma_i = 1$ for $i = 1, 2, \ldots, N$.

A key step in ℓ_1-TV generalization is to reduce the infinite search space $\mathbb{R}^N$ to a finite search space V^N. This can be accomplished through dynamic programming, the basic idea of which is to decompose the problem into a series of similar, simpler, and tractable subproblems. Specifically, we use the Viterbi algorithm [43] to minimize the discrete energy. A critical step of the Viterbi algorithm is to compute the distance transform of the non-uniform mesh induced by V. We further use $Val(y)$ to denote the set of values of N-tuple y, namely

$$Val(y) = \left\{ v : 1 \le i \le N, y_i = v \right\} \tag{3}$$

We can minimize ℓ_1-TV problems whose values are contained in the $Val(y)$ values of the signal data y. Our goal is to minimize this form of energy generalization:

$$E(u_1, \ldots, u_N) = \alpha \sum_{i=1}^{N-1} d(u_i, u_{i+1}) + \sum_{i=1}^{N} \gamma_i d(u_i, y_i)$$

where $u_1, \ldots, u_N$ can take the values in the finite set $V = \left\{ v_1, \ldots, v_K \right\}$, where K denotes the number of distinct values in the data. The Viterbi algorithm solves this problem in two steps: tabulation of energies and reconstruction by backtracking.

For the tabulation step, the starting point is the table $G^1 \in \mathbb{R}^K$ given by

$$G_k^1 = \gamma_1 d(v_k, y_1), \quad k = 1, 2, \ldots, K \tag{4}$$

where K represents the cardinality of V. For $i = 2, \ldots, N$, we compute $G^i \in \mathbb{R}^K$ by

$$G_k^i = \gamma_i d(v_k, y_i) + \min_l \left\{ G_l^{i-1} + \alpha d(v_k, v_l) \right\} \tag{5}$$

when G_k^i denotes the energy value of the minimization operator on the data $(y_1, \ldots, y_i)$ with endpoints equal to v_k.

For the backtracking step, an auxiliary tuple $l \in \mathbb{N}^N$ storing minimization indices can be introduced. We initialize the last term of l with $l_N = \arg\min_k G_k^N$ and then compute the corresponding term in l for $i = N-1, N-2, \ldots, 1$ by the following equation:

$$l_i = \arg\min_k G_k^i + \alpha d(v_k, v_{l_{i+1}}) \tag{6}$$

Finally, we reconstruct a minimum $\hat{u}$ from the indices in l, and $\hat{u}$ is the global minimum of the energy:

$$\hat{u}_i = v_{l_i}, \quad i = 1, 2, \ldots, N \tag{7}$$

The time-critical part of Viterbi's algorithm is the computation of the minima:

$$D_k = \min_l G_l + \alpha |v_k - v_l|, \quad k = 1, 2, \ldots, K \tag{8}$$

This problem is called the distance transformation with respect to the ℓ_1-norm distance (weighted by α). In our setup, V is usually a non-uniform grid. Specifically, we use a K-dimensional ascending vector v (i.e., $v_1 < v_2 < \cdots < v_K$) to determine the elements in V. Since the logarithm of the number of values K is smaller than the length of the data N, there is an $O(K \log K) \subset O(KN)$ in time complexity. This is why the proposed ℓ_1-TV algorithm is fast in running time. Algorithm 1 shows the pseudo-code for the real-valued distance transform algorithm of the signal.

Algorithm 1 Signal distance transformation $S(G, v, \alpha)$

Input: $G \in \mathbb{R}^K$, $v \in \mathbb{R}^K$ sorted in ascending order, $\alpha > 0$.
Output: Distance transform D

```
D ← G
for k = 2 to K, k = k + 1 do
    D_k = min(D_{k−1} + α(v_k − v_{k−1}), D_k) via (8)
end for
for k = K − 1 to 1, k = k − 1 do
    D_k = min(D_{k−1} + α(v_k − v_{k−1}), D_k) via (8)
end for
return D
```

By repeating the above formulas and algorithms, one can obtain the final $\hat{u}$. The final estimated signal is $\hat{u}$, which is the denoised signal, in other words, the step signal. The above part is the first part of ℓ_1-TV minimization, i.e., the part that edge-regularizes the noise in the signal. The following is the second part of ℓ_1-TV minimization, i.e., the homomorphic regularization of the signal data.

Remark 1. In detail, we set $\alpha = 1, 2, \ldots, m$ and perform the signal noise regularization marginalization stage cyclically under different values of α. Finally, we count the number of steps J_α in the loop for each α value of the step signal. The step count vector $\hat{y} = \{J_1, J_2, \ldots, J_m\}$ is generated. As a result, the observed signal is transformed into a step count vector with parameter α. It is no longer disturbed by the difference in signal length, and the signal length is fixed to the maximum value of α. This is equivalent to the processing of data cleaning and data missing values, thus making the signal data become normalized and regularized. The complete procedure is described in Algorithm 2.

2.3. Discriminative neural network

To automatically judge whether the aircraft is structurally healthy, we design a regression neural network by taking step count vectors and labels. The architecture of the network is shown in Fig. 5. To be specific, $X_{m\times1}$ denotes the input vector, $A^{[1]} \cdots A^{[10]}$ denote the vectors in shared hidden layers. $a^{[1]}{}_1$ denotes the first network node in the layer $A^{[1]}$, while $a^{[1]}{}_n$ is the nth network node in the layer $A^{[1]}$. The other layers are represented similarly. $B^{[15]}$ denotes the vectors after the processing of five specific hidden layers. $b_1{}^{[16]}$ and $b_2{}^{[16]}$ represent the prediction and determination vectors of the labeled values of the output

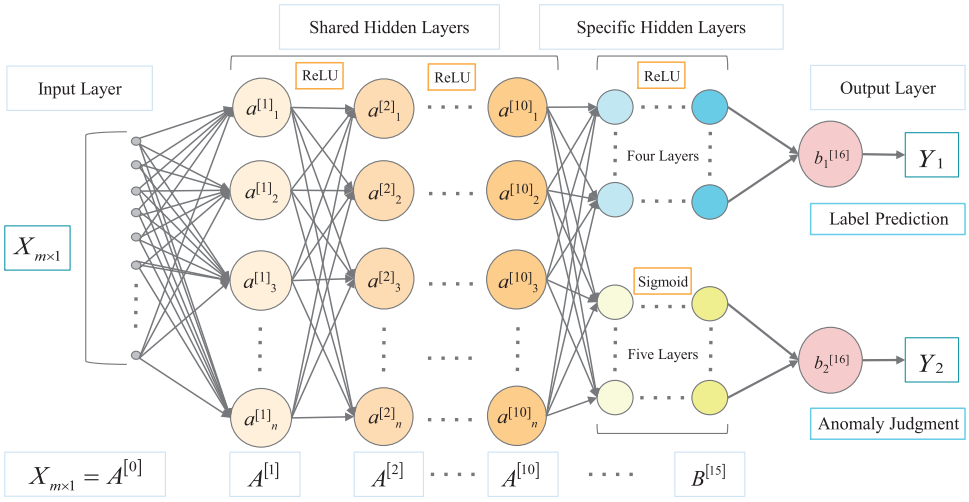

Fig. 5. Architecture of discriminative neural network.

Algorithm 2 ℓ_1-TV minimization

Input: Strain signal $y \in \mathbb{R}^N$, the maximum value m of $\alpha > 0$, and (fixed) weights $\gamma \in (\mathbb{R}_0^+)^N$.
Output: Step signal $\hat{u}$ and step count vector $\hat{y}$

Initialize V with y via (3)
$v \leftarrow K$-tuple of elements of V, sorted ascendingly
for $k = 1$ to K, $k = k + 1$ **do**
  $G_k^1 \leftarrow \gamma_1 d(v_k, y_1)$ via (4)
end for
for $i = 2$ to N, $i = i + 1$ **do**
  $D \leftarrow S(G^i, v, \alpha)$ via Algorithm 1
  for $k = 1$ to K, $k = k + 1$ **do**
    $G_k^i \leftarrow \gamma_i d(v_k, y_i) + D_k$ via (5)
  end for
end for
for $i = N - 1$ to 1, $i = i - 1$ **do**
  $l \leftarrow \arg\min_{k=1,\cdots,K} G_k^i + \alpha d(v_k, \hat{u}_{i+1})$ via (6)
  $\hat{u}_i \leftarrow v_{l_i}$ via (7)
end for
return $\hat{u}$
$\alpha \leftarrow 1$
while $\alpha \leq m$ **do**
  Initialize $J_\alpha = 0$
  for $i = 1$ to $N - 1$ **do**
    if $\hat{u}(i+1) \neq \hat{u}(i)$ **then**
      $J_\alpha = J_\alpha + 1$
    end if
  end for
  $\alpha = \alpha + 1$
end while
Generate $\hat{y} = \{J_1, J_2, \cdots, J_m\}$

layer, respectively. $\hat{Y}_1$ and $\hat{Y}_2$ are the final predicted labeled values and signaled determination values of the output layer, respectively. ReLU and Sigmoid denote two different types of activation functions, respectively. Their formulations can be found in [44].

We use strain step signals as nodes in the input layer. As Fig. 5 shows, the number of nodes is fixed to m, which is the maximum value of α. We choose ten hidden layers as shared hidden layers to extract the shared feature coarse-grained representation of the strain step signal, where ReLU is utilized as the activation function of each layer. The output layer needs to predict both the signal label value and whether the signal anomaly occurs. Before that, we need to design two task-specific hidden layers separately to extract the specific feature fine-grained representations of the strain step signal under different tasks. For the prediction of the signal label value, we design a specific hidden layer with four hidden layers and use ReLu as the activation function of each layer. For the judgement of signal anomaly, we design specific hidden layers containing five hidden layers and use Sigmoid as the activation function of each layer.

Finally, we describe the selection of loss functions. For the prediction of signal label value, we select the appropriate regression loss function, i.e., mean square error (MSE) loss function. It is defined as

$$\mathrm{MSE} = \frac{1}{m}\sum_{i=1}^{m}(x_i - \hat{x}_i)^2$$

where m is the number of samples, x_i denotes the actual value, and $\hat{x}_i$ denotes the predicted value. For the judgement of signal anomaly, we select the loss function suitable for binary classification, i.e., binary cross-entropy loss function. In the model training, we use the stochastic gradient descent method [45] to minimize the loss functions.

3. Experimental study

Previously, we introduce the proposed methodology in detail. In this section, we conduct experiments to verify the effectiveness and efficiency of the proposed scheme. All experiments are performed on an HP desktop machine and a single server. The HP desktop features a 2.50 GHz Intel i7-11700F processor, 16 GB RAM of memory and a 12 GB NVIDIA GeForce RTX 3060 graphics card of video memory. The configuration of the server is 2.40 GHz Intel fifth generation to strong processor E5-2680-v4 and 424G, NVIDIA GeForce RTX 3090 video memory. In the following, we introduce the performance of each stage in the proposed scheme.

3.1. Dataset description

Aircraft structural strain signal data are very difficult to obtain, and they mainly come from real industrial applications. We collect and construct two stain signal datasets for structural fatigue damage, which contains both signal data and label data. All datasets are derived from real strain sensor measurements of two aircraft types (A and B), which are provided by Aviation Industry Corporation of China. The type-A dataset consists of 6000 pieces. The average length of each strain signal is around 4000. The type-B dataset consists of 500 pieces. The average length of each strain signal is around 3500. In order to increase

the size of type-B dataset, we perform its virtual expansion, including signal slicing and flipping, to generate similar signals. We employ experts to label the generated virtual signal one by one. Finally, we expand the size of type-B data to 3000. The relevant dataset parameters are summarized in Table 1, which include the range of operating conditions, sampling period, signal length, and signal count.

Table 1
Description of dataset parameters.

Aircraft type	Operating condition	Sampling period	Signal length	Signal count
Type-A	11 010 101–14 200 502	5 s	3750–4050	6000
Type-B	11 240 103–13 260 502	20 s	3450–3550	3000

3.2. Determination of noise type

At this stage, we analyze noise distribution characteristics in structural strain signals, thus resulting in determination of noise type. Here we employ six classic signal filtering methods, i.e., mean filtering, median filtering, Gaussian filtering wavelet analysis, 3σ rule [46], and median absolute deviation, to reveal the signal variation trend. These methods can be invoked directly from Matlab toolbox. The filtering results are shown in Fig. 6(b)–(g). We merge all the results in Fig. 6(h). It zoomed view is covered in Fig. 6(i).

Whereafter, we analyze and extract the signal features. As seen from Fig. 7, we find that there are two main noise types in observed signals. The one shows random, continuous small fluctuations in the signals, which called tiny hairy signals (Gaussian-like noise). The other presents isolated pulse or bright spots in the signals, i.e., abnormal or extreme values that appears suddenly, which called single signals with anomalous movements in peak and valley areas (impulse-like noise).

3.3. Signal preprocessing

At this stage, we preprocess observed signals by applying eight filtering methods, i.e., mean filtering, median filtering, Gaussian filtering, linear regression, quadratic regression, robust linear regression, robust quadratic regression, and least squares filtering, as shown in Fig. 8. Based on the comparison results, we see that the least squares filtering method has the best smoothing effect since strain signals contain tiny hairy signals (Gaussian-like noise), as analyzed in Section 3.2. In addition, impulse-like noise is eliminated to some extent since noise range $[X, Y]$ is optimal. Therefore, we use least squares filtering to preprocess noise in strain signals.

3.4. Precise signal noise removal and classification

This stage is the core of the proposed scheme, which aims to transform complex strain signals into simple step ones, thus resulting precise signal noise removal and classification. Before applying the total variational method, we use proportional sampling for preprocessed signals while the signal variation trend is consistent before and after sampling. As a result, the data complexity is reduced as much as possible. After the performance of the total variational method, we conduct expert judgements to analyze the strain jump signal and other special circumstances and then classify them, thus generating labels to construct training and test sets.

To be specific, we set the step length from 1 to 20 in the proportional sampling. After the traversal, we choose the appropriate step length based on all sampling results. Our selection criterion is that the sampled signal can contain all the bumps in the original signal. When it holds, the biggest step length is the best. Note that the absolute value of the difference between the bump signal value and mean value of the

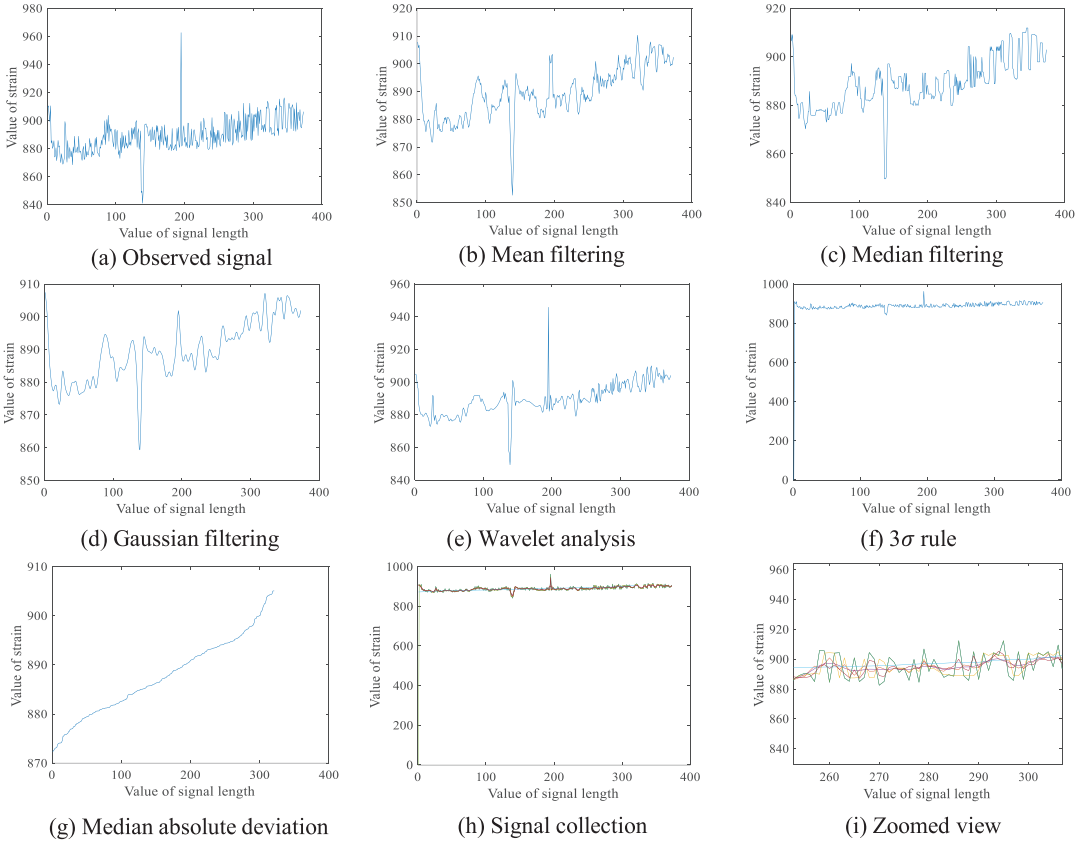

Fig. 6. Strain signal filtering results.

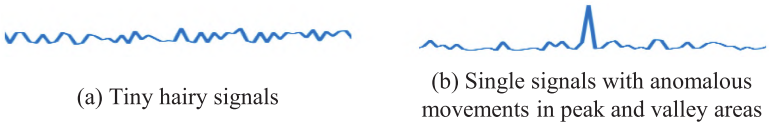

(a) Tiny hairy signals

(b) Single signals with anomalous movements in peak and valley areas

Fig. 7. Noise types in strain signals.

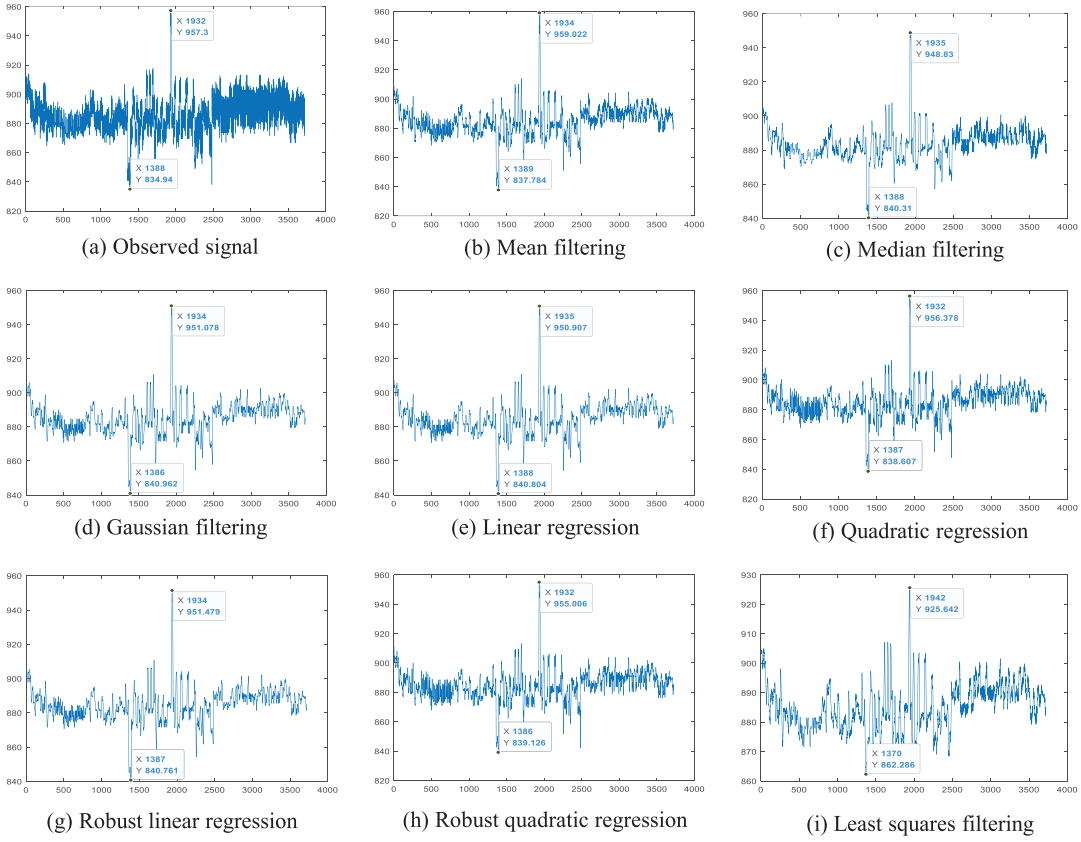

Fig. 8. Results of eight signal preprocessing methods.

signal is greater than or equal to 60. Experimental results show that the optimal sampling step length is 9 on type-A dataset and 4 on type-B dataset. After sampling, the variational method is applied to remove signal noise, thus forming a collection of step signals with different values of parameter α. Here, we carry out the traversal of α from 1 to m being manually preset. We count the number of steps J_α in the loop for each α value of the step signal. Thus, the step count vector $\hat{y} = \{J_1, J_2, \ldots, J_m\}$ is generated. A typical example is shown in Fig. 9.

3.5. Signal discrimination

Based on the step count vector and labels, we train a discriminative neural network designed in Section 2.3. For type-A dataset, we use 70% of it, i.e., 4200 strains signals, to train the network. For type-B dataset, we use 80% of it, i.e., 2400 strain signals, to train the network. Since the data structure of the type-B dataset is more complex and varied than type-A's, we use more data in type-B dataset to train the discriminative network model. The output of the network indicates the judgment of whether the signal is normal or not. Finally, we select the remaining 30% of the type-A dataset and 20% of the type-B dataset as testing data.

3.6. Comparative experiment

In order to demonstrate the superiority of the proposed scheme, we compare it with six same-type signal denoising and anomaly judgment methods including deep learning and traditional methods often used in the industry, namely, Dynamic thresholding (DT) [47], 3σ rule [46], LSTM-FCN [40], TS2Vec [41], OS-CNN [38], and DSN [37]. We conduct experiments on type-A and type-B datasets. The network settings and data amount selection are consistent with ones on discriminative neural networks and anomaly judgments presented in the above two subsections. The dynamic threshold of abnormal judgment is set to 120. The comparison results on judgment accuracy are summarized in Table 2.

As Table 2 indicates, the proposed scheme is superior to other peers. The reason why other peers show poorer results is that the data structure of aircraft strain signals is complex. The better results are obtained on type-A dataset, which is due to the fact that the strain signals in the dataset are less disturbed by noise during generation and transmission. However, the strain signals in type-B data are more affected by noise during the generation and transmission process. By seeing Table 2, we can easily find that the proposed scheme achieves greatly higher judgment accuracy than six peers. This is since employs multiple strategies, i.e., noise distribution estimation, variational denoising, expert

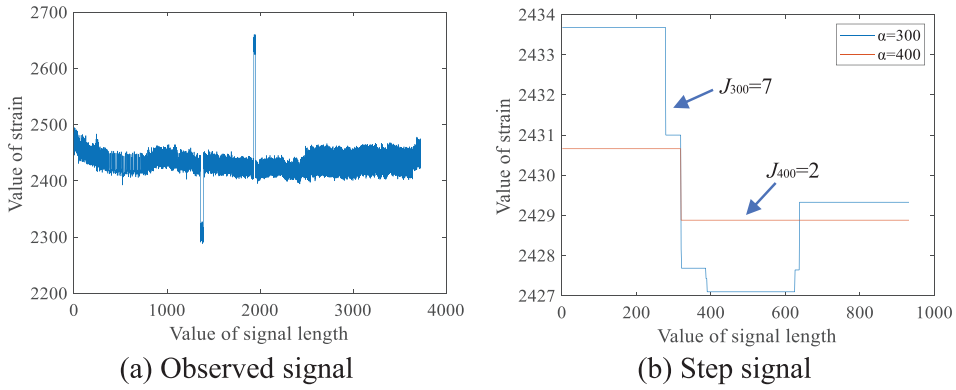

Fig. 9. Denoising results of the variation method.

Table 2
Comparison results on type-A and type-B datasets.

Method	Type-A (%)	Type-B (%)
DT	65.3	49.7
3σ rule	73.6	56.8
LSTM-FCN	88.2	71.3
TS2Vec	90.6	74.6
OS-CNN	91.4	76.2
DSN	92.8	77.5
Ours	**97.7**	**91.8**

judgment and training learning. Therefore, it is concluded that the proposed scheme is suitable for strong noise or outlier removal and judging anomalies in strain signals.

3.7. Computational efficiency and scalability

After calculation and analysis, the proposed scheme judges a signal every 0.83 s on average when the discriminant neural network model is fully trained. Obviously, its computational efficiency is high, which is easy to be extended to practical systems. In addition, it can be extended, such as replacing better discriminant neural networks, to further improve the signal discrimination accuracy. From Table 2, we also see that the proposed scheme has better experimental results on both types of aircrafts than other traditional and deep-learning methods. In conclusion, the proposed scheme has strong scalability.

4. Conclusion

In order to solve the dilemma of structural strain signal processing in the whole machine fatigue test at present, this work propose a fast and robust multi-strategy scheme for structural health monitoring. In this scheme, a statistical analysis method is reported to analyze noise characteristics in strain signals. It is concluded that the noise is a mixture of Gaussian-like (tiny hairy signals) and impulse-like noise (single signals with anomalous movements in peak and valley areas). By signal preprocessing and precise noise removal, we transform the complex strain signals into simple step ones. The proposed variational method plays a crucial role during the process. As a result, whether the aircraft is structurally healthy is accurately judged. Finally, a discriminative neural network is proposed to realize automatic signal discrimination. Experimental results reported for two real-world datasets demonstrate that the proposed scheme is effective and efficient. However, there are still several problems worth solving in the future work. The proposed scheme can be packaged into a system module that can be loaded on the aircraft. In addition, it is offline and cannot process strain data in real time, which needs to be further improved.

CRediT authorship contribution statement

Cong Wang: Methodology, Formal analysis, Data curation, Conceptualization. **Xin Tan:** Software, Methodology, Investigation. **Xiaobin Ren:** Resources, Project administration, Conceptualization. **Xuelong Li:** Supervision.

Declaration of competing interest

The authors declare the following financial interests/personal relationships which may be considered as potential competing interests: Xiaobin Ren reports a relationship with Shaanxi Neifu Zhongfei Airport Management Co., Ltd. that includes: employment. Xuelong Li reports a relationship with Institute of Artificial Intelligence (TeleAI), China Telecom. that includes: employment. If there are other authors, they declare that they have no known competing financial interests or personal relationships that could have appeared to influence the work reported in this paper.

Data availability

No data was used for the research described in the article.

References

[1] C. Zhang, A.A. Mousavi, S.F. Masri, G. Gholipour, K. Yan, X. Li, Vibration feature extraction using signal processing techniques for structural health monitoring: A review, Mech. Syst. Signal Process. 177 (2022) 109175.
[2] S. Das, P. Saha, S.K. Patro, Vibration-based damage detection techniques used for health monitoring of structures: A review, J. Civil Struct. Health Monit. 6 (3) (2016) 477–507.
[3] K. Kluger, Fatigue life estimation for 2017A-T4 and 6082-T6 aluminum alloys subjected to bending-torsion with mean stress, Int. J. Fatigue 80 (2015) 22–29.
[4] A.K. Vasudevan, K. Sadananda, N. Iyyer, Fatigue damage analysis: Issues and challenges, Int. J. Fatigue 82 (2016) 120–133.
[5] L. Qiu, S. Yuan, Q. Wang, Y. Sun, W. Yang, Design and experiment of PZT network-based structural health monitoring scanning system, Chinese J. Aeronaut. 22 (5) (2009) 505–512.
[6] P. Park, P. Di Marco, J. Nah, C. Fischione, Wireless avionics intracommunications: A survey of benefits, challenges, and solutions, IEEE Internet Things J. 8 (10) (2021) 7745–7767.
[7] D. Goyal, B.S. Pabla, The vibration monitoring methods and signal processing techniques for structural health monitoring: A review, Arch. Comput. Methods Eng. 23 (4) (2016) 585–594.
[8] M. Kordestani, M.E. Orchard, K. Khorasani, M. Saif, An Overview of the state of the art in aircraft prognostic and health management strategies, IEEE Trans. Instrum. Meas. 72 (2023) 1–15.
[9] A. Sanchez, J. Pablo, H. Adeli, Signal processing techniques for vibration-based health monitoring of smart structures, Arch. Comput. Methods Eng. 23 (2016) 1–15.
[10] H.A. Richard, M. Sander, Fatigue crack growth in real structures, Int. J. Fatigue 50 (2013) 83–88.

[11] K. Vamvoudakis-Stefanou, J. Sakellariou, S. Fassois, Vibration-based damage detection for a population of nominally identical structures: Unsupervised Multiple Model (MM) statistical time series type methods, Mech. Syst. Signal Process. 111 (2018) 149–171.
[12] V. Giurgiutiu, A. Zagrai, J. Bao, Piezoelectric wafer embedded active sensors for aging aircraft structural health monitoring, Struct. Health. Monit. 1 (1) (2002) 41–61.
[13] Y. Wei, F. Gao, Architecture design method for structural health monitoring system (SHM) of civil aircraft, in: 2017 Int. Conf. Sensing, Diagnostics, Prognostics, and Control, 2017, pp. 736–739.
[14] S. Ren, et al., Structural health monitoring system and experiment study of aircraft tapered pipeline structure, in: 2020 Int. Conf. Sensing, Diagnostics, Prognostics, and Control, 2020, pp. 347–352.
[15] Y. Wang, S. Hu, T. Xiong, Y. Huang, L. Qiu, Recent progress in aircraft smart skin for structural health monitoring, Struct. Health. Monit. 21 (5) (2022) 2453–2480.
[16] L. Qiu, S. Yuan, P. Liu, W. Qian, Design of an all-digital impact monitoring system for large-scale composite structures, IEEE Trans. Instrum. Meas. 62 (7) (2013) 1990–2002.
[17] H. Fu, Z. Sharif Khodaei, M.H.F. Aliabadi, An event-triggered energy-efficient wireless structural health monitoring system for impact detection in composite airframes, IEEE Internet Things J. 6 (1) (2019) 1183–1192.
[18] F.M. Reis, P.F. da Costa Antunes, N.M. Mendes Maia, A.R. Carvalho, P.S. de Brito André, Structural health monitoring suitable for airborne components using the speckle pattern in plastic optical fibers, IEEE Sens. J. 17 (15) (2017) 4791–4796.
[19] Y. Zhou, D. Liu, D. Li, Y. Zhao, M. Zhang, W. Zhang, Review on structural health monitoring in metal aviation based on fiber bragg grating sensing technology, in: 2020 Prognostics and Health Management Conference, 2020, pp. 97–102.
[20] A. Al-Salah, S. Zein-Sabatto, M. Bodruzzaman, M. Mikhail, Two-level fuzzy inference system for aircraft's structural health monitoring, in: 2013 Proceedings of IEEE Southeastcon, 2013, pp. 1–6.
[21] M. Ciminello, Distributed fiber optic for structural health monitoring system based on auto-correlation of the first-order derivative of strain, IEEE Sens. J. 19 (14) (2019) 5818–5824.
[22] B. Du, C. Lin, L. Sun, Y. Zhao, L. Li, Response prediction based on temporal and spatial deep learning model for intelligent structural health monitoring, IEEE Internet Things J. 9 (15) (2022) 13364–13375.
[23] C. Wang, W. Pedrycz, Z. Li, M. Zhou, J. Zhao, Residual-sparse fuzzy c-means clustering incorporating morphological reconstruction and wavelet frame, IEEE Trans. Fuzzy Syst. 29 (12) (2021) 3910–3924.
[24] W. Liu, J. Liu, C. Hao, Y. Gao, Y. Wang, Multichannel adaptive signal detection: Basic theory and literature review, Sci. China Inf. Sci. 65 (2022) 121301.
[25] Y. Lv, W. Zhao, Z. Zhao, W. Li, K.H. Kam, Vibration signal-based early fault prognosis: Status quo and applications, Adv. Eng. Inform. 52 (2022) 101609.
[26] Y. Chen, H. Li, T.D. Wang, K.R. Oldham, Improved extended kalman filter estimation using threshold signal detection with an MEMS electrostatic microscanner, IEEE Trans. Ind. Electron. 67 (2) (2020) 1328–1336.
[27] C. Wang, J. Yang, W. Pedrycz, M. Zhou, Z. Li, Wavelet frame-based fuzzy c-means clustering for segmenting images on graphs, IEEE Trans. Cybern. 50 (9) (2020) 3938–3949.
[28] C. Wang, W. Pedrycz, Z. Li, M. Zhou, Kullback–Leibler divergence-based fuzzy c-means clustering incorporating morphological reconstruction and wavelet frames for image segmentation, IEEE Trans. Cybern. 52 (8) (2022) 7612–7623.
[29] Z. Huang, X. Zeng, D. Wang, S. Fang, Noise reduction method of nanopore based on wavelet and kalman filter, Appl. Sci. 12 (19) (2022) 9517.
[30] C. Wang, W. Pedrycz, Z. Li, M. Zhou, S.S. Ge, G-image segmentation: similarity-preserving fuzzy c-means with spatial information constraint in wavelet space, IEEE Trans. Fuzzy Syst. 29 (12) (2021) 3887–3898.
[31] S. Gao, I.W. Tsang, L. Chia, Sparse representation with kernels, IEEE Trans. Image Process. 22 (2) (2013) 423–434.
[32] L. Liu, L. Chen, C.L.P. Chen, Y.Y. Tang, C.M. pun, Weighted joint sparse representation for removing mixed noise in image, IEEE Trans. Cybern. 47 (3) (2017) 600–611.
[33] C. Chen, L. Liu, L. Chen, Y. Tang, Y. Zhou, Weighted couple sparse representation with classified regularization for impulse noise removal, IEEE Trans. Image Process. 24 (11) (2015) 4014–4026.
[34] M. Elforjani, S. Shanbr, Prognosis of bearing acoustic emission signals using supervised machine learning, IEEE Trans. Fuzzy Syst. 65 (7) (2018) 5864–5871.
[35] S.M. Patole, M. Torlak, D. Wang, M. Ali, Automotive radars: A review of signal processing techniques, IEEE Signal Process. Mag. 34 (2) (2017) 22–35.
[36] B.Z. Cunha, C. Droz, A. Zine, S. Foulard, M. Ichchou, A review of machine learning methods applied to structural dynamics and vibroacoustic, Mech. Syst. Signal Process. 200 (2023) 110535.
[37] Q. Xiao, B. Wu, Y. Zhang, S. Liu, M. Pechenizkiy, E. Mocanu, D.C. Mocanu, Dynamic sparse network for time series classification: Learning what to see, in: 36th Adv. Neural Inf. Process. Syst, 2022, pp. 16849–16862.
[38] W. Tang, G. Long, L. Liu, T. Zhou, M. Blumenstein, J. Jiang, Omni-scale CNNs: A simple and effective kernel size configuration for time series classification, in: 10th Int. Conf. Learn. Represent, 2022, pp. 1–17.
[39] H. Lu, L. Jin, X. Luo, B. Liao, D. Guo, L. Xiao, RNN for solving perturbed time-varying underdetermined linear system with double bound limits on residual errors and state variables, IEEE Trans. Ind. Inform. 15 (11) (2019) 5931–5942.
[40] F. Karim, S. Majumdar, H. Darabi, S. Chen, LSTM fully convolutional networks for time series classification, IEEE Access 6 (2018) 1662–1669.
[41] S. Azodolmolky, et al., Ts2vec: Towards universal representation of time series, in: 36th AAAI Conf. Artif. Intell, 2022, pp. 1–20.
[42] W.-S. Lu, S.-C. Pei, C.-C. Tseng, A weighted least-squares method for the design of stable 1-D and 2-D IIR digital filters, IEEE Trans. Signal Process. 46 (1) (1998) 1–10.
[43] G.D. Forney, The viterbi algorithm, Proc. IEEE 61 (3) (1973) 268–278.
[44] D. Yarotsky, Error bounds for approximations with deep ReLU networks, Neural Netw. 94 (2017) 103–114.
[45] S. Amari, Backpropagation and stochastic gradient descent method, Neurocomputing 5 (4–5) (1993) 185–196.
[46] F. Pukelsheim, The three sigma rule, Am. Stat. 48 (2) (1994) 88–91.
[47] T. Li, M. Comer, E. Delp, J.L. Mathieson, R.H. Foster, M.W. Chan, A stacked predictor and dynamic thresholding algorithm for anomaly detection in spacecraft, in: 38th IEEE Int. Conf. Military Communications, 2019, pp. 165–170.

Cong Wang received the B.S. degree in automation and the M.S. degree in mathematics from Hohai University, Nanjing, China, in 2014 and 2017, respectively. He received the Ph.D. degree in mechatronic engineering from Xidian University, Xi'an, China in 2021.

He is now an Associate Professor in the School of Artificial Intelligence, OPtics and ElectroNics (iOPEN), Northwestern Polytechnical University, Xi'an, China. He was a Visiting Ph.D. Student at the Department of Electrical and Computer Engineering, University of Alberta, Edmonton, AB, Canada, and the Department of Electrical and Computer Engineering, National University of Singapore, Singapore. He was also a Research Assistant at the School of Computer Science and Engineering, Nanyang Technological University, Singapore. His current research interests include wavelet analysis and its applications, fuzzy theory, granular computing, as well as image processing.

Xin Tan received the B.S. degree in computer science and technology from Chengdu University of Technology, Chengdu, China in 2021. He received the M.S. degree in computer technology at Northwestern Polytechnical University, Xi'an, China in 2024. His current research interests include image segmentation, noise analysis, and signal processing.

Xiaobin Ren received the B.S. degree from Guizhou University of Finance and Economics, Guiyang, China, in 2009, the M.S. degree from Xi'an Jiaotong University, Xi'an, China, in 2020, and the Ph.D. degree from Lyceum of the Philippines University, Philippines, in 2023.

He is now a General Manager of Shaanxi Neifu Zhongfei Airport Management Co., Ltd., Xi'an, China. His current research interests include machine learning image processing, and aviation weapon equipment test.

Xuelong Li is currently a Full Professor with the Institute of Artificial Intelligence (TeleAI), China Telecom Corp Ltd, Beijing, China.